



Nonlinear Hammerstein model of ultrasonic motor for position control using differential evolution algorithm

Song Lu, Shi Jingzhuo*

Henan University of Science and Technology, Luoyang 471023, China

ARTICLE INFO

Keywords:

Ultrasonic motor
Hammerstein model
Identification
Differential evolution algorithm

ABSTRACT

The model of ultrasonic motor (USM) is the foundation of the analysis and control of the motor. Ultrasonic motor maintains nonlinear and complicated in dynamics due to its special structure and unique operating, which makes it difficult to establish a good model with traditional modeling. Moreover, the model should be established in line with strong nonlinearities. The nonlinear Hammerstein model of USM is established in this paper, which can better characterize the nonlinear motor. To adapt the model to the need of position control of ultrasonic motor, driving frequency and rotor position are considered as the input and output variables of the Hammerstein model respectively. To improve the accuracy of model and the efficiency of modeling process, model identification combined with differential evolution algorithm is designed. The comparison of model calculation results with the experimental data shows the accuracy of the established model and the validity of the proposed modeling.

1. Introduction

Due to the special operation mechanism of ultrasonic motor (USM), it operates with obvious nonlinear and time-varying characteristics leading to difficulty in obtaining ideal motion performance. In order to meet the application requirements of USM, on the one hand, many analysis and research works on the nonlinear operation mechanism of USM is deepening [1–5]. And various methods are used to improve the operation characteristic of USM [6,7] or propose new motor structure [8–13]. On the other hand, appropriate control method can also obviously improve the operation performance of USM. The model of USM is the foundation of the design of control method. It is a premise to improve the control performance of USM when the motor model is suitable for control applications and remains accurate enough. In recent years various methods have been put forward for the modeling of USM, such as theoretical model [1,2,7,8], equivalent circuit model [14], finite element analysis model [15–17] and kinds of control models [18–27]. In general, all of these models are mathematical models. Theoretical model is derived from the theoretical analysis of the motor's operation. However, the structure of theoretical model remains rather complicated due to the difficulty in precisely describing the piezoelectric energy conversion and mechanical friction transmission. Its model form is usually accurate, but there are too many undetermined parameters that are difficult to determine specific values and time-varying, which limits its actual precision. Limited by the characteristics

of the basic circuit components, the equivalent circuit model describes the dynamic process of the ultrasonic motor too rough, so it is difficult to obtain a more precise model form. Equivalent circuit model can be used for the overall analysis of its performance, but the internal variables and local properties of ultrasonic motor are difficult to describe and the dynamic performance is poor. Finite element analysis model can be used for designing motor structure and has higher accuracy. However, due to the large amount of calculation and limited by the expression and use of the model, it is difficult to be used in other occasions such as motor motion control.

The control models of ultrasonic motor mainly include neural network models [18,19] and identified models [20–22]. Appropriate forms of neural network can be used to fit any of the input-output relationship. Therefore, the characteristics of ultrasonic motor can also be expressed by neural network. As we all know, the excitation function and its structure are main factors affecting neural network mapping relationships. Since the matching degree of excitation function and nonlinear characteristics of ultrasonic motor are low, the structure of the neural network is usually complex and the form of neural network is not idiomatically mathematical model. Although neural network can be directly used for ultrasonic motor's neural network control system, there are still other problems in for designing controller. Therefore, the identification model based on experimental data is mostly used in ultrasonic motor control.

Today most of the identification models of ultrasonic motor are

* Corresponding author.

E-mail address: sjznew@163.com (S. Jingzhuo).

linear because classical system identification is usually of linear models. A linear model with variable parameters can be used for fitting ultrasonic motor so as to improve the model accuracy [21]. However, it will make the structure of the model complicated and make it increasingly difficult for designing controller. Thus, nonlinear identification models are proposed in ultrasonic motor's modeling. In [22], a linear model of the motor is obtained by least squares identification considering the friction between the stator and rotor, then the nonlinear parameter model which reflects the friction part has been achieved by quadratic interpolation method based on the nonlinear friction theory. Despite the great complexity in model structure, the friction theory used in modeling is a beneficial attempt. In [23–27], the nonlinear Hammerstein model has been introduced to ultrasonic motor modeling as well as the speed control. The pioneering work of Bigdeli [23] and Zhang [24] has been considered in this field. They have the proposals of using Hammerstein model to describe the nonlinearities of the speed characteristics verse driving voltage amplitude of the ultrasonic motor. In [23], the steady-state nonlinear part is derived from a polynomial function fitting of the steady-state data, which reflects mechanical properties of ultrasonic motor. Since these data is unable to present the nonlinearities completely, the simulation results have indicated that the model is less accurate. In [25], the Hammerstein model is also based on the steady state data. Thus, there is a great limitation in predicting the dynamic characteristics of the motor. In [26], the nonlinear part of the Hammerstein model is fitted by a radial basis function neural network which leads to a complicated model. In [23–26], the linear dynamic part of the Hammerstein model is directly set to be a first-order inertia link without any modeling. As a result, the dynamic characteristics of ultrasonic motor were not expressed completely and the model is less accurate. Meanwhile, the linear part and the nonlinear part of the Hammerstein model modeling independently would result in a large model error in general. In [27], the nonlinear Hammerstein model based on particle swarm optimization algorithm has been established in ultrasonic motor's speed control. The model is more accurate while the modeling optimization is rather time-consuming.

Above all, there are two major tasks in ultrasonic motor's control modeling. Firstly, how to design an appropriate model better describing the nonlinearities is the key to improve its accuracy. Secondly, in order to acquire sufficient accuracy for model, more undetermined parameters should be provided. So an appropriate model structure is required to ensure the effectiveness of modeling.

The two questions will be discussed in this paper. For the first time, the nonlinear Hammerstein model of ultrasonic motor for position control is established. New model identification method for ultrasonic motor using improved differential evolution algorithm is designed to improve the accuracy of the model. The comparison of model calculation results with the application results shows the validity of the proposed model.

2. The nonlinear Hammerstein model

The operation of traveling-wave ultrasonic motor consists of electro-mechanical energy conversion driven by the ultrasonic vibration of piezoelectric elements and the mechanical friction between the stator and rotor. It leads to serious nonlinearities when ultrasonic motor is running. Motor model is the base to design ultrasonic motor controller. Conventional ultrasonic motor models usually are linear which can not represent the nonlinear characteristics essentially. Besides, the linear model will decrease its accuracy. The actual performance of the motor will deviate from our expectation if the model is inexact. In order to improve the control performance, it is necessary to find a better model which can fully represent the motor.

The nonlinear model of ultrasonic motor can be considered firstly due to its' overtness of the nonlinearities. The Hammerstein model is widely used in nonlinear control fields. The basic structure of the Hammerstein model is shown in Fig. 1, which consists of a static

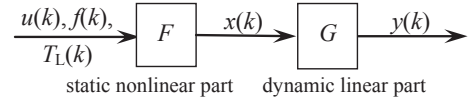


Fig. 1. Structure of the single-input single-output Hammerstein model.

nonlinear part, followed by a dynamic linear part. As shown in Fig. 1, F is the static nonlinear part described by a polynomial function and G is the dynamic linear part expressed by a difference transfer function so as to make the controller easily designed. The input variable is the driving frequency $u(k)$ and the output variable is the angle of the rotation of the motor shaft $y(k)$, $x(k)$ is the unpredictable intermediate variable. Relationships among the variables above can be expressed as shown in Eq. (1).

$$\begin{cases} x(k) = F(u(k)) = r_0 + r_1 u(k) + r_2 u^2(k) + \dots + r_p u^p(k) \\ A(z^{-1})y(k) = z^{-d}B(z^{-1})x(k) \\ A(z^{-1}) = 1 + a_1 z^{-1} + a_2 z^{-2} + \dots + a_m z^{-m} \\ B(z^{-1}) = b_0 + b_1 z^{-1} + b_2 z^{-2} + \dots + b_n z^{-n} \end{cases} \quad (1)$$

wherein d refers to time delay, and $d = 1$, $r_0, r_1, \dots, r_p, a_1, a_2, \dots, a_m, b_0, b_1, \dots, b_n$ are the undetermined parameters; p is the order of nonlinear polynomial function; m and n are orders of $A(z^{-1})$ and $B(z^{-1})$, respectively.

Ultrasonic motor has obvious nonlinearity. From the perspective of motor application, the nonlinear performance of ultrasonic motor is that the relationship between the operating state of the motor (rotational speed, rotation angle) and the variable affecting the operating state is nonlinear. This nonlinearity is most obvious in the speed characteristic of the motor, as shown in the measured characteristic curve in Figs. 2 and 3. There are several variables that can be used to change the operating state of motor. On the one hand, motor operating state is directly related to the electrical parameters of the driving voltage of the ultrasonic motor. These electrical parameters include the frequency, amplitude and phase difference of the driving voltage. In order to improve the efficiency of the motor, the phase difference between two phase driving voltage is set to 90° . Fig. 2 shows the relationship among the other two variables and the rotational speed. It can be seen that the change of frequency and voltage amplitude will lead to the change of rotational speed, and the relationship is not linear. To show this nonlinear relationship more clearly, Fig. 3 shows the characteristic relationship between frequency and rotational speed. On the other hand, the operating state of the ultrasonic motor is also affected by the load torque, and they also present nonlinear relationship.

In the Hammerstein model, the nonlinearity of the ultrasonic motor is expressed by the static nonlinear part of the model. In order to obtain

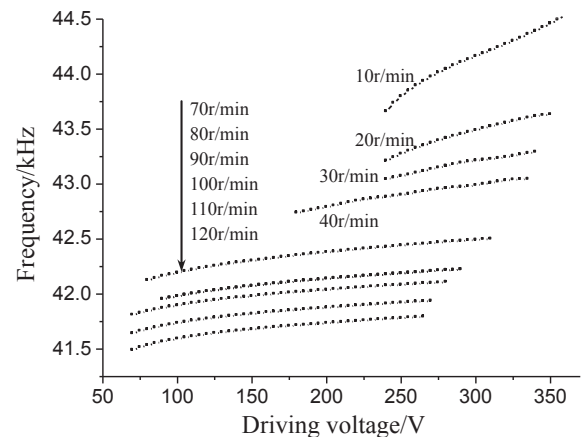


Fig. 2. USM's nonlinear characteristics with different frequency and voltage amplitude (0.1 Nm).

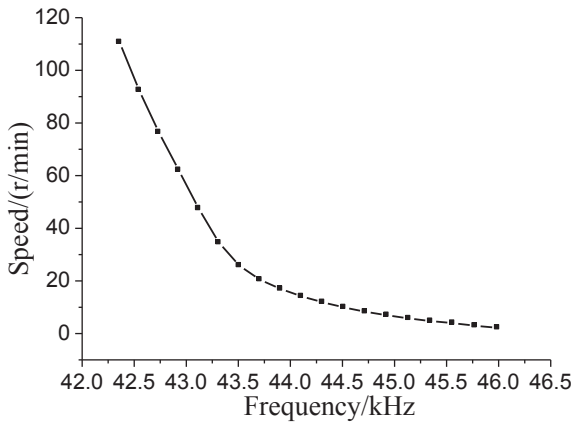


Fig. 3. Frequency nonlinear characteristic of USM (0.1 Nm).

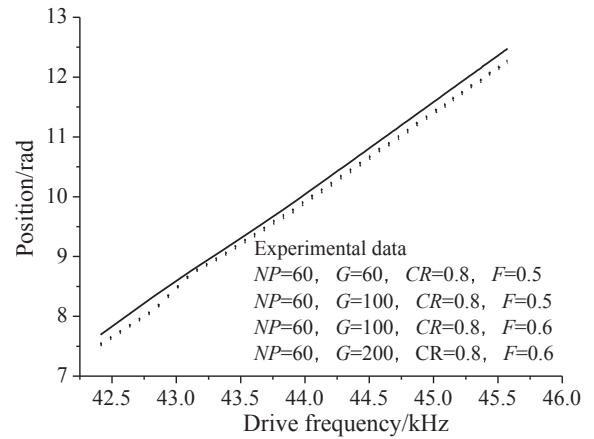


Fig. 5. Comparison between calculation results of the model identification and the experimental data ($m = 2, n = 1$).

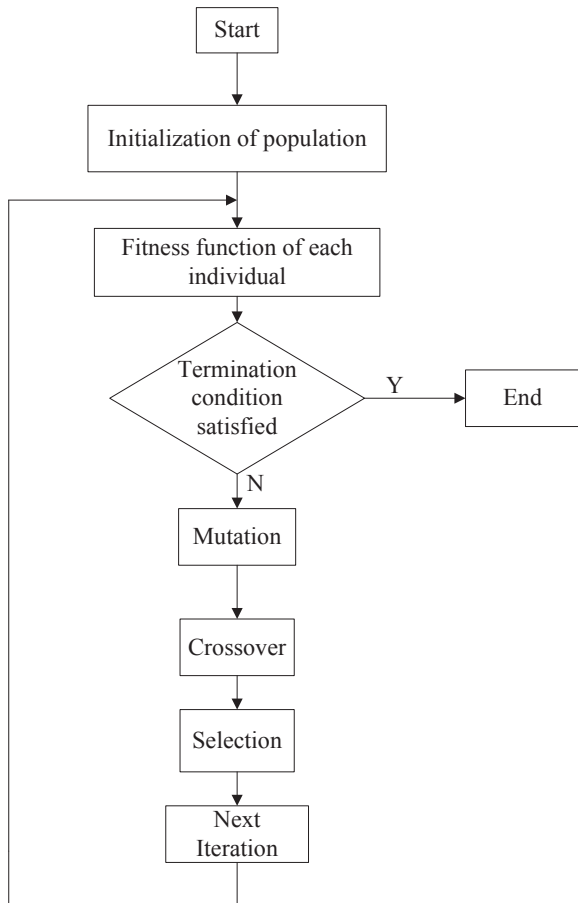


Fig. 4. Flowchart of the proposed differential evolution algorithm.

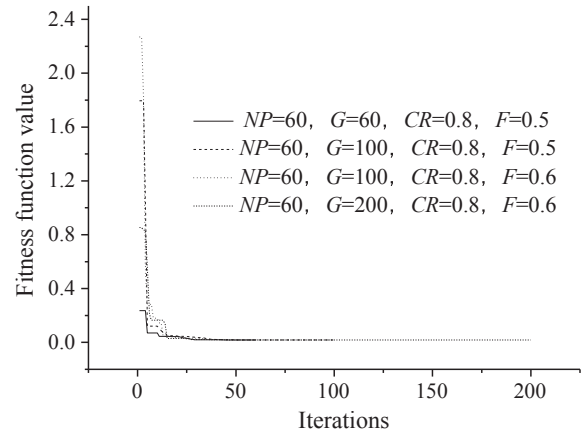


Fig. 6. Fitness function changing curves with different parameters ($m = 2, n = 1$).

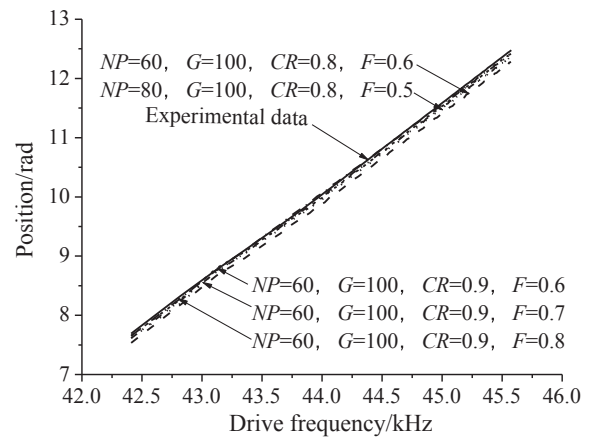


Fig. 7. Comparison between calculation results of the model identification and the experimental data ($m = 2, n = 2$).

Table 1
Parameters of differential evolution algorithm.

Parameter	Initial value	Final value
NP (Population)	60	60
T (Maximum iterations)	100	100
CR (Crossover probabilities)	0.8	0.9
F (mutation probabilities)	0.6	0.7

a static nonlinear partial expression that can better describe the nonlinear characteristics of the ultrasonic motor, the motor speed characteristic data under different load torques, different driving voltage amplitudes and different driving voltage frequencies are measured.

There is an integral relationship among rotational speed and motor rotation angle or position. The integral action in the dynamic element of the Hammerstein model converts the rotational speed into positional information. Figs. 2 and 3 show the measured data curve of the load torque of 0.1 Nm. This paper attempts to fit the above characteristic data with different forms of function. It shows that the expression form shown in Eq. (2) can be better matched with the measured nonlinear characteristic data. Therefore, the Hammerstein model of the ultrasonic

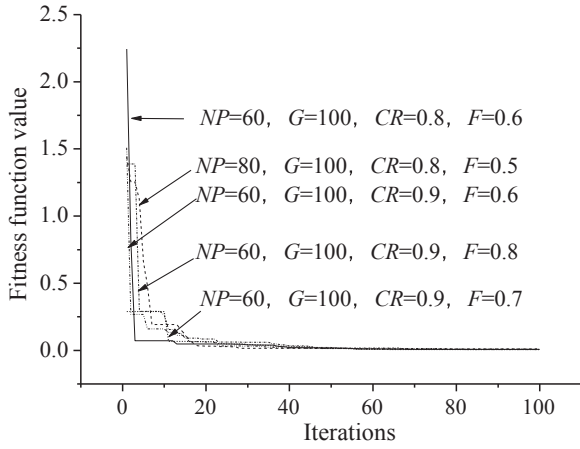


Fig. 8. Fitness function changing curves with different parameters ($m = 2$, $n = 2$).

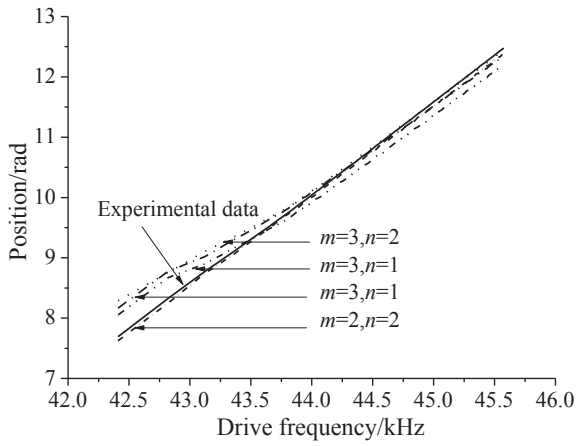


Fig. 9. Comparison of model identification with different model orders.

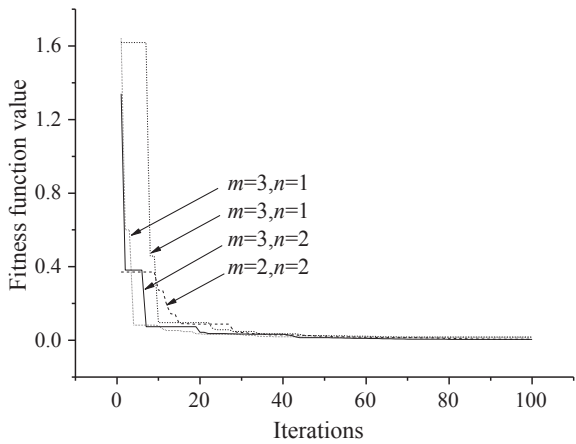


Fig. 10. Fitness function changing curves with different model orders.

motor described in this paper adopts Eq. (2) as the expression of the static nonlinear part of the model.

$$x(k) = r_0 + (r_{u0} + r_{u1}u(k) + r_{u2}u^2(k)) \frac{275.50}{4(f(k) - 42.201)^2 + 2.3648} + r_{T1}T_L(k) + r_{T2}T_L^2(k) \quad (2)$$

wherein u is the amplitude of the ultrasonic motor driving voltage; f is the frequency of the motor driving voltage; T_L is the load torque of the motor; r_0 , r_{u0} , r_{u1} , r_{u2} , r_{T1} and r_{T2} are unknown parameters and the value

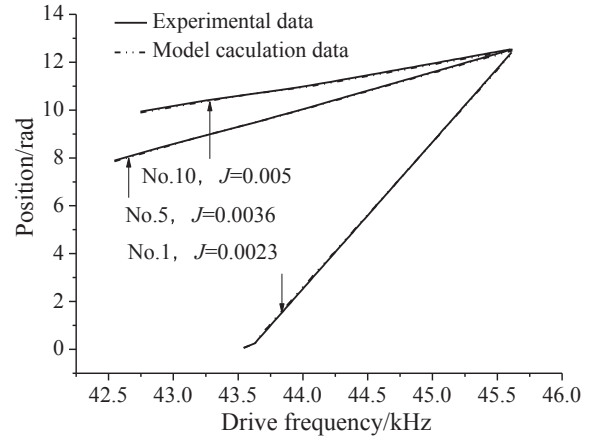


Fig. 11. Comparison of model calculation results and the experimental data (data for modeling, $m = 3$, $n = 2$, $p = 1$).

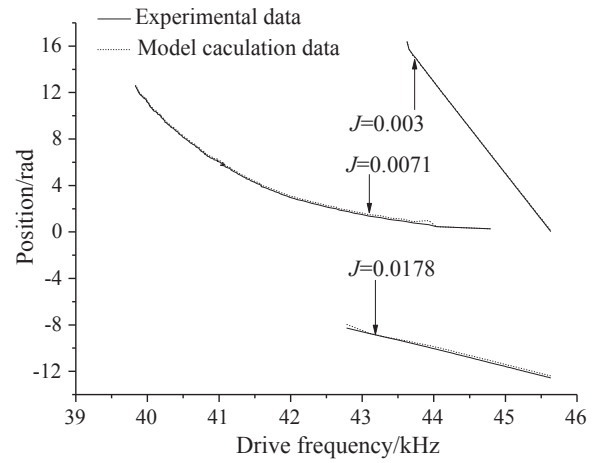


Fig. 12. Comparison of model calculation results and the experimental data (data for validating, $m = 3$, $n = 2$, $p = 1$).

is identified by optimization algorithm.

The nonlinear Hammerstein model of USM will be established if the parameters (r_0 , r_{u0} , r_{u1} , r_{u2} , r_{T1} , r_{T2} , a_1 , a_2, \dots, a_m , b_0 , b_1, \dots, b_n) are determined. Usually, the system identification is used for model parameters. In fact, the system identification is an optimization based on experimental data. Namely, the optimal parameters are determined if the identification model is best close to experimental result by trying different model parameter values. During this process, fitness function should be introduced to evaluate the error of model calculation results and the experimental data. In this paper, the mean square error of model calculation results and the experimental data are set as the fitness function during identification.

$$J = \sum_{i=1}^q \left[\sqrt{\frac{\sum_{k=1}^h [y_{ir}(k) - y_i(k)]^2}{h}} \right] / q \quad (3)$$

wherein $y(k)$ is the model calculation data, $y_r(k)$ is the measured data, q is the number of measured data sequence for identification, h is the number of data in each measured data sequence. Apparently, the smaller of fitness function J , the less difference between the model calculation results and the experimental data. Thus, model identification aims at finding the minimum value of the fitness function on the premise that the Eq. (1) is determined.

In order to find an exact model, the experiment data used in modeling should reflect the operating of ultrasonic motor as much as possible. The driving frequency and the rotor position are measured when

Table 2
Error of model calculation results and the experimental data.

No.	1	2	3	4	5	6	7	8	9
Mean square error	0.0023	0.0037	0.0036	0.0036	0.0036	0.004	0.0045	0.0043	0.004
maximum absolute error (rad)	0.0614	0.0587	0.0694	0.0625	0.0608	0.0593	0.0629	0.0603	0.0598
No.	10	11	12	13	14	15	16	17	18
Mean square error	0.005	0.0078	0.0069	0.0157	0.0262	0.0017	0.0178	0.0071	0.003
maximum absolute error (rad)	0.061	0.1894	0.0803	0.1911	0.4029	0.0406	0.0942	0.3626	0.3186

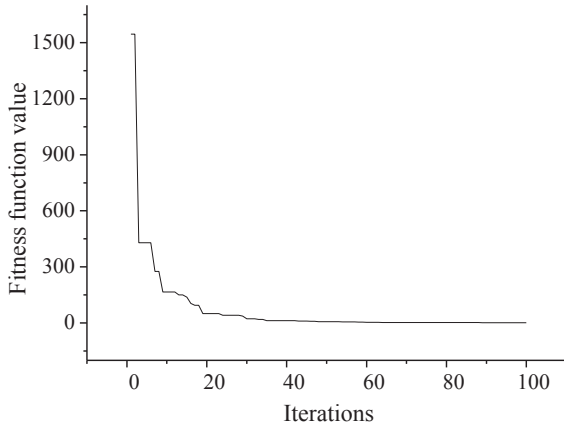


Fig. 13. Fitness function changing curve.

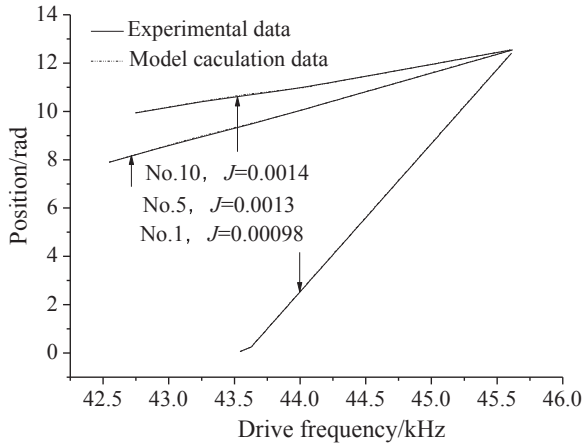


Fig. 14. Comparison of model calculation results and the experimental data (data for modeling, the fitness function is the sum of absolute error).

different reference position values are given. Then we record the experimental data sequences of every reference position. Among all the experimental data, 35 sets of data which cover the available operating range of the motor are selected for model identification. In addition, other 3 sets of data are selected randomly for model validation.

Each set of the experimental data contains all dynamic and steady-state data during the running of the motor. As the major factor required for modeling, the dynamic data reflects the dynamic characteristics of the motor. Steady data means that the motor position control has reached steady state and the motor is almost to stop. In this case, there is no significant change in steady data and the data is just used for reflecting the steady state gain of the motor model. Considering the homogenization in Eq. (3), too much steady-state data will decrease the influence of dynamic data on model parameter identification. As a result, excessive steady-state data of each set is eliminated.

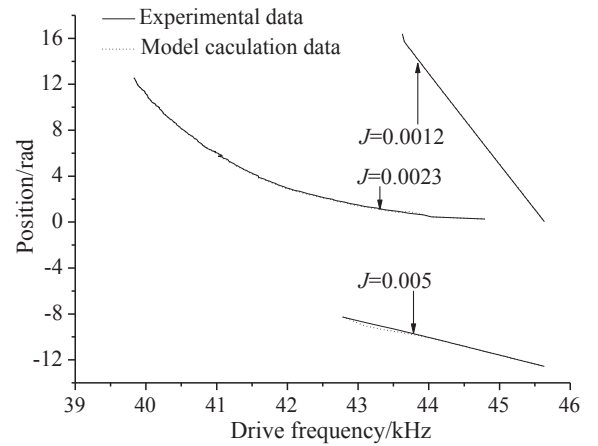


Fig. 15. Comparison of model calculation results and the experimental data (data for validating, the fitness function is the sum of absolute error).

3. The nonlinear Hammerstein modeling of USM based on differential evolution algorithm

Conventional system identification usually uses least square optimization algorithm which is simple and stable for model parameters identification. But this optimization algorithm is poor to deal with complex optimization. Therefore, finding a better optimization algorithm seems to be an effective solution to deal with this problem.

In this paper, we propose a differential evolution algorithm to identify the nonlinear Hammerstein model of ultrasonic motor. Differential evolution (DE) algorithm is an intelligent optimization algorithm which has no special requirements for searching space and has been successfully applied to solve complicated nonlinear problems [28,29]. Compared with ant colony, particle swarm, flora and other intelligent optimization algorithms, differential evolution algorithm is not only astonishingly simple but less identified in its parameters. In another aspect, the robustness of the algorithm as well as the optimization efficiency is improved.

With the genetic algorithm improved, we can obtain differential evolution algorithm [28]. Differential evolution algorithm uses real-valued elements encoding and the replacement operation occurs only when new offspring individuals are superior to that of random individuals of the population. A new generation of individuals is produced by crossover operation of three parent individuals. Thus, the flexibility of the algorithm is increased and a better balance between random search and local optimization is struck.

Differential optimization algorithm mainly consists of mutation, crossover, selection and operations. Prior to the optimization, the initial population and algorithm parameters should be decided firstly. Assuming that the initial population is NP and every individual of the population is generated at random, each individual is of D -dimensional vector, the maximum iterations are T . X_i which represents an arbitrary individual of the population, $i = 1, 2, \dots, NP$. Supposing that the current iterations are G , the current population can be expressed as $P_{X,G} = \{X_{1,G}, X_{2,G}, \dots, X_{NP,G}\}$, $G = 1, 2, \dots, T$. If the initial individual is in the range of $[X_{min}, X_{max}]$, the initial value of i_{th} individual is taken as

Table 3
Error between model calculation results and the experimental data.

No.	1	2	3	4	5	6	7	8	9
Mean square error	0.00098	0.0014	0.0014	0.0012	0.0013	0.0013	0.0015	0.0014	0.0014
maximum absolute error (rad)	0.0273	0.044	0.0421	0.0324	0.0414	0.0409	0.0447	0.0419	0.0332
No.	10	11	12	13	14	15	16	17	18
Mean square error	0.0014	0.0052	0.0019	0.0016	0.0014	0.0025	0.005	0.0023	0.0012
maximum absolute error (rad)	0.0397	0.1555	0.0483	0.0464	0.0416	0.0666	0.0894	0.1649	0.2979

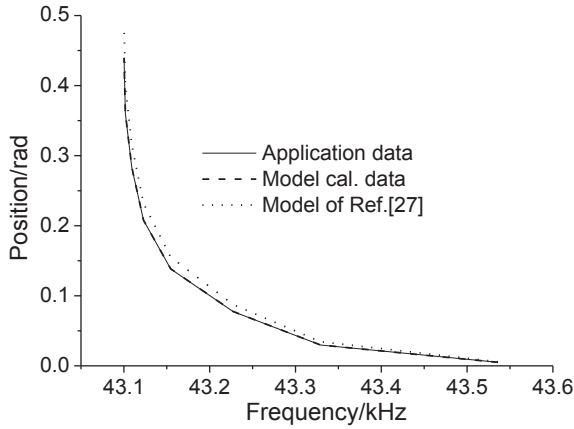


Fig. 16. Comparison of model calculation results and the application results I.

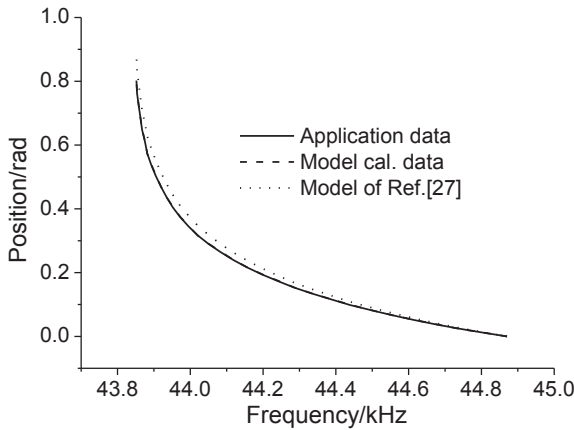


Fig. 17. Comparison of model calculation results and the application results II.

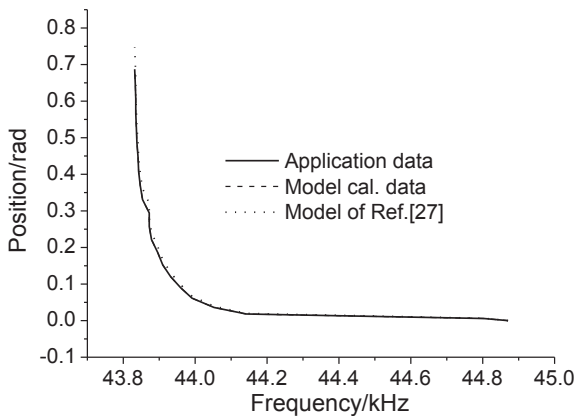


Fig. 18. Comparison of model calculation results and the application results III.

Table 4
Error between model calculation results and the application results.

Model	The proposed model			Model of Ref. [27]		
	Fig. 16	Fig. 17	Fig. 18	Fig. 16	Fig. 17	Fig. 18
Mean square error	0.00026	0.00109	0.00023	0.01666	0.02296	0.01998
maximum absolute error (rad)	0.00073	0.00389	0.00068	0.04704	0.07506	0.06056

follows

$$X_i = X_{min} + rand(1) * (X_{max} - X_{min}), \quad i = 1, 2, \dots, NP \quad (4)$$

wherein $rand(1)$ is generated randomly in the interval $[0, 1]$. The values of individuals are restricted to the feasible solution space which can reduce the blindness of searching as shown in Eq. (4).

Lots of experiences indicate that the population size NP should be 5–10 times more than that of identified parameters. Consequently, a reasonable optimizing efficiency is attained in the premise of population diversity and the identification accuracy is ensured. Vector dimension D is equal to the number of identified parameters.

Small-scale stochastic disturbance is introduced to the population by mutation which can widen the search range to enhance the global searching ability. Specific operations are shown in Eq. (5).

$$X_{i,G+1} = X_{best,G} + F * (X_{o,G} - X_{p,G}), \quad o, p \in [1, NP] \text{ and } o \neq p \neq i \quad (5)$$

wherein X_{best} is the optimal individual of the current population, X_o and X_p are two random individuals that are different from the current mutation individual X_i , the constant F is the constriction factor. F determines the zoom of the vector error between two random parent individuals, namely, the possible value of stochastic disturbance is limited as well. If F is too small, the algorithm will fall into local optimization. Otherwise, the convergence speed may slow down if the value is too large. Usually, F is a constant in interval $[0.5, 1]$.

Crossover operation is performed after the mutation operation. The vector information of the original individual $X_{i,G}$ and the mutation individual $X_{i,G+1}$ is recombined randomly. Then, a new individual $U_{i,G+1}$ is produced which includes at least one dimension information of the mutation individuals so as to increase the population diversity. Define the crossover operation as follows:

$$\text{If } rand(j) \leq CR \text{ or } j = randn(i), \quad U_{i,j,G+1} = X_{i,j,G+1}, \quad (j = 1, 2, \dots, D)$$

$$\text{If } rand(j) > CR \text{ and } j \neq randn(i), \quad U_{i,j,G+1} = X_{i,j,G}, \quad (j = 1, 2, \dots, D)$$

wherein $U_{i,j,G+1}$ is the j th vector of the new individual $U_{i,G+1}$, $X_{i,j,G+1}$ is the j th vector of the mutation individual $X_{i,G+1}$, $X_{i,j,G}$ is the j th vector of $X_{i,G}$; $rand(j)$ are generated randomly in the interval $[0, 1]$, $randn(i)$ are generated randomly in integer $[1, 2, \dots, D]$, CR is a constant crossover probability which determines the probability of crossover operation. When $CR = 1$, $U_{i,G+1} = X_{i,G+1}$, there is no new individual produced by crossover and the convergence is fast. However, it is easy to fall into local searching when the searching space is decreased. It proves that when $CR \in [0.7, 1]$, there is a better identification result.

The selection operation is used to decide whether the new individual $U_{i,G+1}$ produced by mutation and crossover or the original individual $X_{i,G}$ would be kept when the value of the fitness function of

the new individual $U_{i,G+1}$ is better than $X_{i,G}$, $X_{i,G}$ out of selection and the new individuals are selected for next iteration. Otherwise, the original individuals are selected for next iteration while the new individuals are out of selection. Then the next iteration continues. The flowchart of differential evolution algorithm is shown in Fig. 4.

4. Parameters confirming of differential evolution algorithm

It is crucial to confirm the parameters of differential evolution algorithm used for model identification of USM, so as to obtain better model identification results. The parameters can be adjusted with a specific optimization problem and would directly affect the optimization results.

According to experience, the initial parameters are shown in the second column of Table 1. The model orders of the motor are of $m = 2$, $n = 1$. The fitness function value is 0.0178 after parameters have been identified. Then change the parameters of the DE algorithm, the results indicate that there is little difference in the fitness function values as well as the models. As a result, it is difficult to get a perfect ultrasonic motor model in this case. Take the second set of experimental data for example. The comparison of calculation results of the model identification with the experimental data is shown in Fig. 5. Fig. 6 shows the changing curves of fitness function values during optimization. It is difficult to distinguish the curves with different optimization algorithm parameters as shown in Figs. 5 and 6.

Identify the model parameters when the model orders are of $m = 2$ and $n = 2$. Results show that the convergence is faster and the error between calculation results of the model identification and the experimental data is less than that of case when $n = 1$. It also indicates that the dynamic characteristics of the ultrasonic motor can emerge fully when the model orders are of $m = 2$ and $n = 2$. In this situation, the algorithm parameters are regulating until the optimal solution is found. However, if the maximum iterations go beyond 100, the identification results may be worse. Assume that the maximum iterations are 100. The regulation of population size NP and constriction factor F should agree with the principle of the larger of NP , the smaller of F . When parameters are adjusted to the values shown in the third column of Table 1, the optimal solution achieves. Similarly, take the second set of experimental data for example. Fig. 7 shows the comparison of calculation results of the model identification with the experimental data. Fig. 8 shows the best fitness function changing curves during optimization. Compared with Figs. 5–8, the convergence is faster and the identification is better and model accuracy is greater.

5. The determination of the orders of nonlinear Hammerstein model of USM

The model orders of the ultrasonic motor in this paper is chosen from 1 to 3 taking account of the model accuracy, complexity and control requirements. Differential evolution algorithm is applied to identify the model parameters under different model orders. The comparison of model precision shows that the higher model accuracy, the smaller difference of the fitness function values between identified model and the experimental data. Accordingly, the corresponding model orders are applicable for the actual operating of the ultrasonic motor.

Take the second set of experimental data for example to illustrate the difference among various identified models. Fig. 9 shows the comparison of model calculations with different orders and experimental data. It indicates that the fitting errors of the second group of experimental data is the least when model orders are of $m = 2$, $n = 2$. However, the experimental data of the second group is only one of the whole 15 groups. The final model orders are determined according to the minimum value of the fitness function. Besides, all the experimental data covers the possible operating range of the motor, which should be considered so that the identified model can show the operating of

ultrasonic motor much better. Fig. 10 shows the fitness function convergence curves with different model orders. The results show that when $m = 2$, $n = 2$, the fitness function value is 0.0073. And when $m = 3$, $n = 2$, the minimum fitness function value is 0.006 and the model accuracy of the nonlinear Hammerstein model of USM is the highest at this moment. Thus, the model orders are set as $m = 3$, $n = 2$.

In fact, the process of determining the model orders is to identify model parameters. Therefore, if the model orders of ultrasonic motor are determined, the model identification is finished. The identified model corresponds to the orders of $m = 3$, $n = 2$, and the model parameters are

$$\begin{aligned} a_1 &= -1.5991, & a_2 &= 0.3996, & a_3 &= 0.2082, & b_0 &= 0.1157, \\ b_1 &= -2.1553, & b_2 &= 1.9237, & r_0 &= -1.9213, & r_{u0} &= 0.99006, \\ r_{u1} &= 7.7251E-4, & r_{u2} &= -9.8934E-8, & r_{T1} &= -43.845, \\ r_{T2} &= 3.1163. \end{aligned}$$

Dynamic linear part of the model is

$$x(k) = -1.9213 + (0.99006 + 7.7251E - 4 \cdot u(k) - 9.8934E - 8 \cdot u^2(k)) \cdot \frac{275.50}{4(f(k) - 42.201)^2 + 2.3648} - 43.845T_L(k) + 3.1163T_L^2(k) \quad (6)$$

Nonlinear static part is

$$\frac{y(z^{-1})}{x(z^{-1})} = \frac{0.1157 - 2.1553z^{-1} + 1.9237z^{-2}}{1 - 1.5991z^{-1} + 0.3996z^{-2} + 0.2082z^{-3}} \quad (7)$$

Here, a more detailed data is given to indicate the effectiveness of the identified model. The first, fifth and tenth group of data are selected to make a comparison of calculation results and the experimental data as shown in Fig. 11. Fig. 12 shows the comparison of three sets of the experimental data for model validation and the calculation results. Table 2 shows the mean square error and maximum absolute error of each group data. Thus, the error between the identified model and the experimental data is reflected directly. It is easy to see that the difference between the model and the experimental data is minor and the model accuracy is high.

6. Adjustment of the fitness function and optimization of the model structure

Repeated simulation results show that when the fitness function is the sum of absolute error, a smaller error is received as well as a better tracking performance of the experimental data based on the regulated model parameters. Assume that the population size $NP = 60$, maximum iterations $G = 100$, crossover probabilities $CR = 0.9$, constriction coefficient $F = 0.7$ and the model orders are of $m = 3$, $n = 2$. The convergence rate of the fitness function is shown in Fig. 13.

The comparison of the first, fifth and tenth group of model calculation data and the experimental data is shown in Fig. 14. Fig. 15 shows the calibration results between three groups of model calculation data and the experimental data.

The simulation indicates that the fitting effect of using sum of absolute error is better than using mean squared error and the performance of ultrasonic motor is improved. Therefore, the model parameters can be determined as: $a_1 = -1.7673$, $a_2 = 0.5515$, $a_3 = 0.2155$, $b_0 = 0.003$, $b_1 = 0.276$, $b_2 = -0.2792$, $r_0 = -2.1135$, $r_{u0} = 0.98494$, $r_{u1} = 7.8792E - 4$, $r_{u2} = -9.7858E - 8$, $r_{T1} = -47.379$, $r_{T2} = 3.8363$. And the dynamic linear part of the model is

$$x(k) = -2.1135 + (0.98494 + 7.8792E - 4 \cdot u(k) - 9.7858E - 8 \cdot u^2(k)) \cdot \frac{275.50}{4(f(k) - 42.201)^2 + 2.3648} - 47.379T_L(k) + 3.8363T_L^2(k) \quad (8)$$

Nonlinear static part is

$$\frac{y(z^{-1})}{x(z^{-1})} = \frac{0.003 + 0.276z^{-1} - 0.2792z^{-2}}{1 - 1.7673z^{-1} + 0.5515z^{-2} + 0.2155z^{-3}} \quad (9)$$

In order to compare with Table 2, the mean square error is still used for fitness function as shown in Eq. (4). The maximum absolute error and the fitness function values of each group are collected as shown in Table 3. In this case, the mean square error of the sets of data used for modeling is 0.0017.

In Figs. 16–18, application results (solid lines) are used to test the accuracy of the proposed model. The calculated data (dash lines) of the model are best suited to the application data. The value of mean square error and maximum absolute error are shown in Table 4. As a contrast, the calculated data of the model proposed in Ref. [27] are also drawn in Figs. 16–18. These figures and Table 4 clearly illustrate the improvement of the proposed model. For example, in Fig. 17, the mean square error of the proposed model is 0.00109, but the mean square error of the model proposed in Ref. [27] is 0.02296.

7. Conclusions

This paper proposes the nonlinear Hammerstein model for position control of ultrasonic motor and the differential evolution algorithm is used for model identification. Comparison of the calculation data and the experimental data demonstrates the effectiveness of the model.

Researches show that the effective non-linear Hammerstein model is very appropriate for ultrasonic motor. Besides, the Hammerstein model rather than linear model with variable parameters can be less complex. Various models have been put forward for the modeling of ultrasonic motor, such as theoretical model, equivalent circuit model, finite element analysis model, and so on. They are respectively applicable to different applications. No matter which model form you use, it should be based on an in-depth understanding of the nonlinear characteristics of ultrasonic motor in order to obtain a relatively simple model that can accurately reflect the operating characteristics of ultrasonic motor. Polynomials are used by the Hammerstein model to express the non-linearity of the object. Although it is feasible, it is not necessarily the easiest method. The nonlinear part of the model should be rationally designed according to the specific characteristics of ultrasonic motor.

The key to the success of identification modeling is whether the optimization algorithm is applicable or not. Differential evolution algorithm used for the identification of model orders and model parameters can be less complex as well, modeling efficiency as well as convergence effectiveness can be improved. Under same model parameters, multiple identifications based on differential evolution algorithm can converge to the same optimal solution. It indicates that the robustness of differential evolution algorithm is superior to other intelligent optimization algorithms like GA algorithms which can also include random operations in modeling process of ultrasonic motor.

Acknowledgments

This study was supported by the National Natural Science Foundation of China through grant number U1304501.

References

- [1] Shi Weijia, Zhao Hui, Zhao Bo, Qi Xue, Chen Weishan, Tan Jiubin, Extended optimum frequency tracking scheme for ultrasonic motor, *Ultrasonics* 90 (2018) 63–70.
- [2] Wan Zhijian, Hu Hong, Modeling and experimental analysis of the linear ultrasonic motor with in-plane bending and longitudinal mode, *Ultrasonics* 54 (3) (2014) 921–928.
- [3] Zhang Dongsheng, Wang Shiyu, Xiu Jie, Piezoelectric parametric effects on wave vibration and contact mechanics of traveling wave ultrasonic motor, *Ultrasonics* 81 (2017) 118–126.
- [4] Mizutani Yasuhiro, Higuchi Takayuki, Iwata Tetsuo, Takaya Yasuhiro, Time-resolved oblique incident interferometry for vibration analysis of an ultrasonic motor, *Int. J. Auto. Technol.* 11 (5) (2017) 800–805.
- [5] Lv Qibao, Yao Zhiyuan, Li Xiang, Contact analysis and experimental investigation of a linear ultrasonic motor, *Ultrasonics* 81 (2017) 32–38.
- [6] Wu. Jiang, Mizuno Yosuke, Nakamura Kentaro, Polymer-based ultrasonic motors utilizing high-order vibration modes, *IEEE/ASME Trans. Mech.* 23 (2) (2018) 788–799.
- [7] V. Dabbagh, A.D. Sarhan Ahmed, J. Akbari, N.A. Mardi, Design and manufacturing of ultrasonic motor with in-plane and out-of-plane bending vibration modes of rectangular plate with large contact area, *Measure.: J. Int. Measure. Confederation* 109 (2017) 425–431.
- [8] Wang Liang, Liu Junkao, Liu Yingxiang, Tian Xinqi, Yan Jipeng, A novel single-mode linear piezoelectric ultrasonic motor based on asymmetric structure, *Ultrasonics* 89 (2018) 137–142.
- [9] Mashimo Tomoaki, Urakubo Takateru, Shimizu Yukiharu, Micro geared ultrasonic motor, *IEEE/ASME Trans. Mech.* 23 (2) (2018) 781–787.
- [10] Sanikhani Hamed, Akbari Javad, Design and analysis of an elliptical-shaped linear ultrasonic motor, *Sens. Actuators, A* 278 (2018) 67–77.
- [11] Wang Guangqing, Xu Wentan, Gao Shuaishuai, Yang Binqiang, Lu Guoli, An energy harvesting type ultrasonic motor, *Ultrasonics* 75 (2017) 22–27.
- [12] Liu Jian, Jin Jiamei, Ji Ruinan, Chen Di, A novel modal-independent ultrasonic motor with dual stator, *Ultrasonics* 76 (2017) 177–182.
- [13] Shi Shengjun, Xiong Huaiyin, Liu Yingxiang, Chen Weishan, Liu Junkao, A ring-type multi-DOF ultrasonic motor with four feet driving consistently, *Ultrasonics* 76 (2017) 234–244.
- [14] Mashimo Tomoaki, Micro ultrasonic motor using a one cubic millimeter stator, *Sens. ActuatorsA: Phys.* 213 (2014) 102–107.
- [15] Ri Chol-Su, Kim Myong-Jin, Kim Chol-Su, Im Song-Jin, ‘Study on the vibration displacement distribution of a circular ultrasonic motor stator’, *Ultrasonics* 59 (5) (2015) 59–63.
- [16] I.A. Renteria Marquez, V. Bolborici, A dynamic model of the piezoelectric traveling wave rotary ultrasonic motor stator with the finite volume method, *Ultrasonics* 77 (2017) 69–78.
- [17] I.A. Renteria-Marquez, A. Renteria-Marquez, B.T.L. Tseng, A novel contact model of piezoelectric traveling wave rotary ultrasonic motors with the finite volume method, *Ultrasonics* 90 (2018) 5–17.
- [18] Chen Tien-Chi, Yu Chih-Hsien, Generalized regression neural-network-based modeling approach for traveling-wave ultrasonic motors, *Electr. Power Compon. Syst.* 37 (6) (2009) 645–657.
- [19] F.-J. Lin, Y.-S. Kung, S.-Y. Chen, Y.-H. Liu, Recurrent wavelet-based Elman neural network control for multi-axis motion control stage using linear ultrasonic motors, *IET Electr. Power Appl.* 4 (5) (2010) 314–332.
- [20] Shi Jingzhuo, You Dongmei, Characteristic model of travelling wave ultrasonic motor, *Ultrasonics* 54 (2) (2014) 725–730.
- [21] Liu Bo, Shi Jingzhuo, Model identification on stepping response of ultrasonic motor frequency-speed control, *Micro-Motors* 43 (11) (2010) 77–80.
- [22] Tan Yonghong, Qiu Fumei, Xiao Xinyu, Model identification for rotary travelling wave ultrasonic motor, *Contr. Eng. China* 18 (5) (2011) 806–809.
- [23] Nooshin Bigdeli, Mohammad Haeri, Modelling of an ultrasonic motor based on Hammerstein model structure, in: 2004 8th International Conference on Control, Automation, Robotics and Vision, Kunming, China, December, 2004, 2, pp. 1374–1378.
- [24] Xinliang Zhang, Yonghong Tan, Modelling of ultrasonic motor with dead-zone based on Hammerstein model structure, *J. Zhejiang Univ. Sci. A* 9 (1) (2008) 58–64.
- [25] Jiantao Zhang, Tiemin Zhang, Zhiyang Xie, Wu Wei, Multivariable nonlinear model of ultrasonic motor based on Hammerstein model and uniform design, *Proceeding of the 8th World Congress on Intelligent Control and Automation, Jinan, China, 2010*, pp. 5794–5799.
- [26] Mohammad Jahani, Hamed Mojallalli, Neural network based modeling of travelling wave ultrasonic motor using genetic algorithm, 2010 The 2nd International Conference on Computer and Automation Engineering, Singapore, 2010, pp. 486–490.
- [27] Shi Jingzhuo, Zhao Juanping, Xu Huang Jingtao, Zhang Juwei Meiyu, Zhang Lei, Identification of ultrasonic motor’s non-Linear Hammerstein model, *J. Control, Auto. Electric. Syst.* 25 (5) (2014) 537–546.
- [28] Fan Qinqin, Yan Xuefeng, Differential evolution algorithm with self-adaptive strategy and control parameters for P-xylene oxidation process optimization, *Soft. Comput.* 19 (5) (2015) 1363–1391.
- [29] Saber M. Elsayad, Ruhul A. Sarker, Daryl L. Essam, An improved self-adaptive differential evolution algorithm for optimization problems, *IEEE Trans. Ind. Inf.* 9 (1) (2013) 89–99.